Effect and Correction of Unequal Cable Losses and Dispersive Delays on Delay-and-Sum Beamforming

Q. Liu & S.W. Ellingson

April 25, 2012

This document has been submitted to the IEEE for consideration for publication.

Effect and Correction of Unequal Cable Losses and Dispersive Delays on Delay-and-Sum Beamforming

Q. Liu and S. W. Ellingson

April 25, 2012

Abstract—**Radio frequency beamforming arrays may be vulnerable to distortion caused by cables, especially when the distortion is unequal between sensors. This paper analyzes the effects of unequal per-sensor cable distortion on delay-and-sum beamforming, and proposes methods to equalize the responses using digital FIR filters. A simplified version of the LWA1 radio telescope, consisting of 256 isotropic sensors operating between 10 MHz and 88 MHz, is used as an example. It is shown that unequal and dispersive per-sensor cable response degrades the signal-to-noise ratio (SNR) performance achieved by LWA1 by $0.35-0.86$ dB. It is found that modification of the per-sensor FIR filters used for beamforming delays can reduce this degradation to 0.10 dB at least. A simpler single-frequency correction for loss only is considered, and is also found to be effective.**

Index Terms—**Beamforming, Antenna Array, Radio Astronomy.**

I. Introduction

A common approach to beamforming combines sensor outputs via a delay-and-sum operation. The beamforming delays are selected to equalize the geometrical delays associated with the sensors. Fractional sample period delays can be accurately approximated using finite impulse response (FIR) filters, as described in [1]. However, these systems may be vulnerable to unequal and dispersive responses from physical components such as coaxial cables. Coaxial cable is a commonly-used type of transmission line used in the systems of interest. These cables exhibit frequency-dependent loss and delay. Thus equalization of sensor signals may be required before summing. The effects and equalization of cable loss and dispersion on beamforming have been considered in [2], but the equalizer was designed by trial and error and the solution was only applicable to narrowband analog signals.

In this paper, we describe the problem of unequal cable losses and dispersive delays, analyze the effects on delay-and-sum beamforming, and propose a solution using per-sensor cable correction FIR filters. The designs are considered in the context of the LWA1 radio telescope [3]. However, this work is applicable to a variety of systems which suffer from unequal cable losses and dispersive delays; e.g., sonar arrays [4], HF/VHF band riometers [5], radar arrays [6], and other radio telescopes such as MWA [7], SKA [8], and LOFAR [9].

The theory of digital delay-and-sum beamforming is described in Section II. The primary issue is obtaining the coefficients of the delay FIR filter. The frequency response of a coaxial cable is derived in Section III-A. The primary difficulty in determining the correction filter is inverting the frequency response of the cable. Our approach uses a three-term Taylor series approximation as explained in Section III-B.

For an array consisting of N sensors, there are two candidate strategies to combine delay-and-sum beamforming and equalization of unequal cable losses and dispersive delays: the "concatenation" scheme shown in Figure 1, and the "combination" scheme shown in Figure 2. For the n^{th} sensor, the combination approach uses a single FIR filter $H_n(\omega)$ to simultaneously perform the functions of $H_{cn}^{-1}(\omega)$ and $H_{bn}(\omega)$; where $H_{cn}^{-1}(\omega)$ is used to correct the attenuation and dispersive delay in the cable connected with sensor n, and $H_{bn}(\omega)$ provides the geometrical delay for the delay-and-sum beamforming. The combination scheme has the potential to yield a smaller overall filter length, possibly also resulting in a corresponding reduction in implementation complexity, power consumption, and cost. For these reasons, the combination scheme is investigated in Section IV.

The effectiveness of proposed designs are demonstrated in Section V using LWA1 as an application example. LWA1 operates at frequencies between 10 MHz and 88 MHz using receivers having noise figure of about 2.7 dB [3]. It is shown that unequal cable distortion between sensors significantly degrades the array SNR performance and the proposed correction scheme is beneficial in this case. We also confirm that the combination scheme can improve the array SNR performance with smaller filter length, as opposed to the concatenation scheme.

II. Delay-and-Sum Beamforming

A delay-and-sum beamformer generates the desired beam by delaying the signal from each sensor by an appropriate amount and then summing them together. Typically, the delay associated with the individual sensor is determined by the array geometry and the desired pointing direction. Consider a coordinate system in which the incident direction ψ is represented as $\{\theta, \phi\}$, where θ is the angle measured from the $+z$ axis, and ϕ is the angle measured from the $+x$ axis toward the $+y$ axis. The delay of the signal incident from ψ at the n^{th} sensor is

$$\tau_n(\psi) = -\frac{x_n \sin\theta\cos\phi + y_n \sin\theta\sin\phi + z_n\cos\theta}{c} \ , \quad (1)$$

where c is the speed of light in free space, and (x_n, y_n, z_n) are the coordinates of the n^{th} sensor.

For a given sample period T_s, the time delay D can be interpreted as

$$D = dT_s + \tau \ , \quad (2)$$

where dT_s is the integer sample period delay (coarse delay) with d being an integer, and τ is the fractional sample period

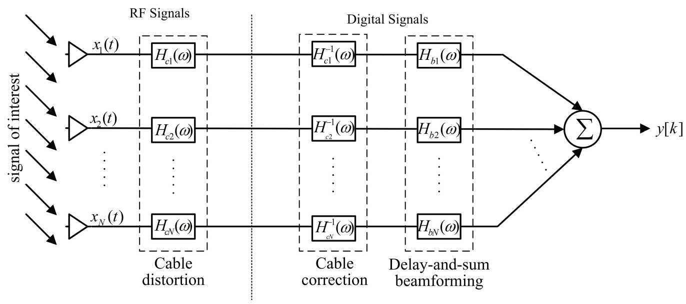

Fig. 1. Concatenation scheme.

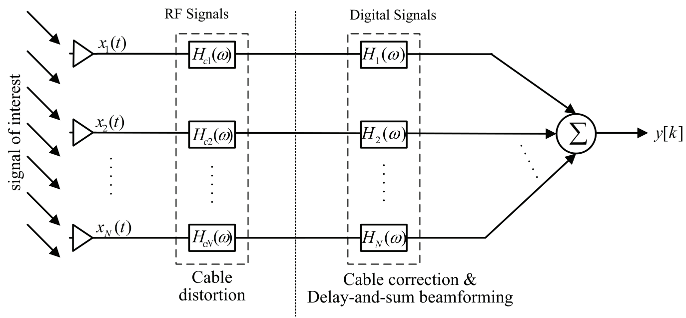

Fig. 2. Combination scheme.

delay (fine delay) satisfying $0 \le \tau/T_s \le 1$. An implementation of this scheme for an array consisting of N sensors is shown in Figure 3, where "first in first out" buffers (FIFOs) are used to implement the coarse delay, and per-sensor M-tap FIR filters are used to implement the fine delay. This scheme minimizes the required length of the delay FIR filter.

From the reconstruction theorem, the ideal impulse response for the delay filter is then

$$h[k] = \operatorname{sinc}\left(k - \frac{\tau}{T_s}\right),\ k \in (-\infty, \infty)\ . \tag{3}$$

Reducing the limits of k from $\pm\infty$ to $\lceil \pm(M-1)/2 \rceil$ in order to obtain an implementable filter results in a FIR filter having M taps. We refer to this as the "prototype truncation" method. This method is affected by Gibbs phenomenon. The resulting frequency domain ripple may be undesirable in many applications (and, in particular, radio spectroscopy).

A simple method to reduce Gibbs phenomenon is by windowing the impulse response. The mainlobe width and sidelobe level depend on the window function and the associated parameters. A comprehensive review of window functions was presented by Harris (1978) [10]. The Kaiser window and the Chebyshev window are two candidates we consider for delay FIR filter designs: The Kaiser window allows control of the peak ripple using one parameter, and the Chebyshev window minimizes the sidelobe level for a given mainlobe width.

An alternative design method is minimax optimization, in which one minimizes the maximum error in the frequency response over the bandwidth of interest. Let $H_i(\omega)$ be the frequency response of the ideal filter. The pseudocode for the minimax optimization is shown in Algorithm 1.

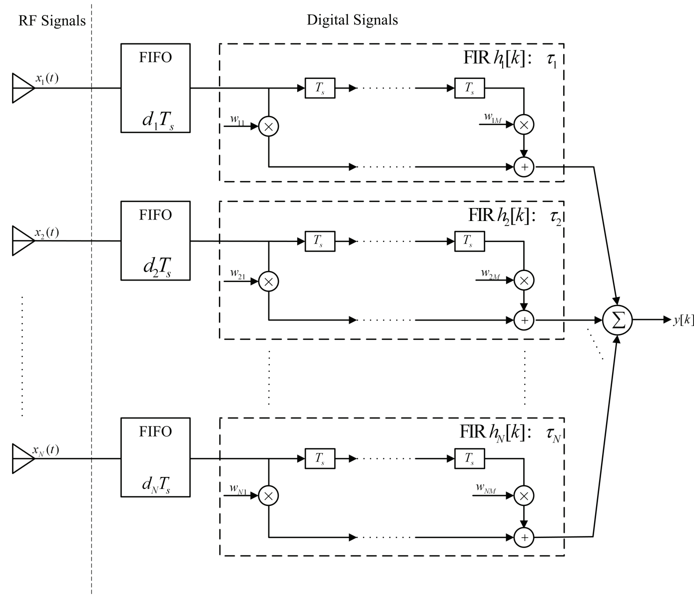

Fig. 3. Block diagram of delay-and-sum beamforming. T_s is the sample period.

Algorithm 1

1: Given $H_i(\omega)$, ΔM, M_0, ϵ, f_s, and Ω

2: $\mathbf{h}_0 \leftarrow \mathcal{F}^{-1}\{H_i(\omega)\}$ followed by sampling

3: Truncate $\mathbf{h}_0$ to M_0 taps

4: Obtain M_0-tap $\mathbf{h}_1$ using

$$\min\left\{\max_{\omega\in\Omega}\left|\sum_{k=0}^{M_0-1} h_1(k)e^{-jk\frac{\omega}{f_s}} - H_i(\omega)\right|\right\}$$

5: $H_1(\omega) \leftarrow \mathcal{F}\{\mathbf{h}_1\}$

6: **if** $\max_{\omega\in\Omega} |\angle H_1(\omega) - \angle H_i(\omega)| > 1.0^\circ$ **then**

7: $\quad M_0 \leftarrow M_0 + \Delta M$, and go to step 4

8: **else if** $\max_{\omega\in\Omega} |\angle H_1(\omega) - \angle H_i(\omega)| \le (1.0^\circ - \epsilon)$ **then**

9: $\quad M_0 \leftarrow M_0 - \lfloor \Delta M/2 \rfloor$, and go to step 4

10: **else if** $(1.0^\circ - \epsilon) < \max_{\omega\in\Omega} |\angle H_1(\omega) - \angle H_i(\omega)| \le 1.0^\circ$ **then**

11: $\quad M_1 \leftarrow M_0$, $\mathbf{h}_1$ is found as M_1 taps

12: $\quad$**return**

13: **end if**

In this algorithm, M_0 is the initial filter length, ΔM is the step size for each iteration, ϵ is the tolerance of the phase error (0.01° is suggested), f_s is the sampling frequency, and Ω is the frequency range of interest.

In this paper, we will focus on the use of windowing and minimax optimization methods for the design of FIR filters.

III. Cable Loss and Dispersive Delay

Coaxial cable is a commonly-used type of transmission line, consisting of inner conductor, insulator, metal layer, outer conductor, and jacket. The source of distortion in coaxial cables is that the center conductor and shield are not perfectly conductive, so that part of the current travels in the metal where power can be dissipated and propagation speed is frequency-dependent [11].

A. Frequency Response of Coaxial Cables

An infinitesimal length of electrical transmission line can be modeled as a resistance (R in Ω/m) and inductance (L in $\mathrm{H/m}$) in series, and a capacitance (C in $\mathrm{F/m}$) and conductance (G in $\mathrm{S/m}$) in parallel [11]. If properly terminated at both ends of the transmission line, the transfer function from the input voltage (i.e., the voltage at the beginning of the transmission line) to the output voltage (i.e., the voltage at distance l) is

$$H(\omega) = e^{-\gamma l} \ , \tag{4}$$

where $\gamma = \sqrt{(R + j\omega L)(G + j\omega C)}$ is the "propagation constant". Separating γ into real and imaginary parts $\gamma = \alpha + j\beta$, we have

$$H(\omega) = e^{-\alpha l} e^{-j\beta l} \ , \tag{5}$$

where the first and second factors describe attenuation and phase along the transmission line at distance l, respectively. The delay along the transmission line of length l is then

$$\tau = -\frac{\mathrm{d}\measuredangle H(\omega)}{\mathrm{d}\omega} = \frac{\mathrm{d}\beta}{\mathrm{d}\omega} l \ , \tag{6}$$

which depends on cable length (as expected), but also possibly on frequency.

Ideally, $G \ll \omega C$ and $R \ll \omega L$, and L and C are frequency-invariant. Under these conditions, γ is approximately constant and imaginary-valued. The frequency response of an ideal coaxial cable is thus

$$H_{ic}(\omega) = e^{-j\omega(\sqrt{LC})l} \ , \tag{7}$$

where the magnitude response is unity and the phase response is linear. Hence the ideal coaxial cable has no loss and is dispersionless.

In practice, however, α is non-zero and frequency-dependent, yielding propagation loss; and β is a non-linear function of ω, yielding dispersion due to the frequency-dependent delay indicated in Equation (6). The cable distortion can thus be defined as

$$H_c(\omega) = H(\omega) H_{ic}^{-1}(\omega) = e^{-\alpha l} e^{-j(\beta - \omega\sqrt{LC})l} \ . \tag{8}$$

A derivation of values for α and β is given in the Appendix. From Equation (44) in the Appendix, the loss in a coaxial cable of length l is

$$A = e^{-\zeta l \sqrt{\omega}} \ , \tag{9}$$

and from Equations (44) and (6), the dispersive delay (delay in addition to that implied by the velocity factor) is

$$\tau_d = \frac{\kappa l}{2\sqrt{\omega}} \ . \tag{10}$$

For a given cable, the parameters ζ and κ are constants independent of frequency, having units of $\mathrm{m}^{-1}\ \mathrm{Hz}^{-1/2}$, described in the Appendix.

B. Correction of Cable Distortion

The frequency response of the ideal correction filter for the compensation of cable distortion is from Equation (44),

$$H_{cd}(\omega) = H_c^{-1}(\omega) = e^{(\zeta + j\kappa)l\sqrt{\omega}} \ . \tag{11}$$

The impulse response of the correction filter, $h_{cd}(t)$, is the inverse Fourier transform of $H_{cd}(\omega)$. There is no explicit closed form of the inverse Fourier transform of Equation (11) available. To bypass this problem, we expand "$e^{g\sqrt{\omega}}$" (where $g = (\zeta + j\kappa)l$ is a constant independent of frequency) as a Taylor series to obtain a simpler expression whose inverse Fourier transform is known. As the frequency response of the correction filter is not linear in ω, neither the one-term nor the two-term Taylor series expansion is appropriate in this case. Using a three-term Taylor series to expand "$e^{g\sqrt{\omega}}$" around some frequency ω_c, we obtain

$$\begin{aligned} e^{g\sqrt{\omega}} \cong \Bigg[& \left(\frac{g^2}{8\omega_c} - \frac{g}{8\sqrt{\omega_c^3}} \right) \omega^2 + \left(\frac{3g}{4\sqrt{\omega_c}} - \frac{g^2}{4} \right) \omega + \\ & \left(\frac{g^2 \omega_c}{8} - \frac{5g\sqrt{\omega_c}}{8} + 1 \right) \Bigg] e^{g\sqrt{\omega_c}} \ . \end{aligned} \tag{12}$$

The approximation of $H_{cd}(\omega)$ given in Equation (11) is then

$$H_{cd}(\omega) \cong \widetilde{H}_{cd}(\omega) = c_0 \omega^2 + c_1 \omega + c_2 \ , \tag{13}$$

where

$$c_0 = \left[\frac{(\zeta + j\kappa)^2 l^2}{8\omega_c} - \frac{(\zeta + j\kappa)l}{8\sqrt{\omega_c^3}} \right] e^{(\zeta + j\kappa)l\sqrt{\omega_c}} \ , \tag{14a}$$

$$c_1 = \left[\frac{3(\zeta + j\kappa)l}{4\sqrt{\omega_c}} - \frac{(\zeta + j\kappa)^2 l^2}{4} \right] e^{(\zeta + j\kappa)l\sqrt{\omega_c}} \ , \tag{14b}$$

$$c_2 = \left[\frac{(\zeta + j\kappa)^2 l^2 \omega_c}{8} - \frac{5(\zeta + j\kappa)l\sqrt{\omega_c}}{8} + 1 \right] e^{(\zeta + j\kappa)l\sqrt{\omega_c}} \ . \tag{14c}$$

The time domain filter $\tilde{h}_{cd}(t)$ for the correction of cable distortion can be obtained by taking the inverse Fourier transform of Equation (13). If sampled at the rate of f_s in the time domain, the correction filter $\widetilde{\mathbf{h}}_{cd}$ in terms of its taps k, is:

$$\begin{aligned} \tilde{h}_{cd}[k] = & \frac{j(c_0^*\pi^2 f_s^2 + c_1^*\pi f_s + c_2^*)k^2 + (2c_0^*\pi f_s^2 + c_1^* f_s)k - 2jc_0^* f_s^2}{2\pi k^3 e^{j\pi k}} - \\ & \frac{j(c_0\pi^2 f_s^2 + c_1\pi f_s + c_2)k^2 - (2c_0\pi f_s^2 + c_1 f_s)k - 2jc_0 f_s^2}{2\pi k^3 e^{-j\pi k}} + \\ & \frac{j(c_2 - c_2^*)k^2 - (c_1 + c_1^*)f_s k - 2j(c_0 - c_0^*)f_s^2}{2\pi k^3} \ . \end{aligned} \tag{15}$$

C. Example

Kingsignal[1] Part Number KSR200DB cables are used in LWA1. The data sheet indicates that KSR200DB cable has the following characteristics: inner conductor radius $a = 0.56$ mm, outer conductor radius $b = 1.83$ mm, and $C = 80.4$ pF/m. Because the conductivities δ_a and δ_b of the inner and outer conductors, respectively, are not accurately known, we obtain ζ and κ from measurements [12] using Equation (46). It is found from measurements that using Equation (38) taking the real

[1] http://www.kingsignal.com/en

part of the propagation constant $\alpha_0 = 0.00428\ \mathrm{m}^{-1}$ at $f_0 =$ 10 MHz gives an excellent fit (within 0.1 dB at 150 MHz) to the 150 MHz, 450 MHz, and 900 MHz loss values provided in the data sheet. Thus, we have $\zeta = 5.4 \times 10^{-7}\ \mathrm{m}^{-1}\ \mathrm{Hz}^{-1/2}$. Using time-domain reflectometry, the additional dispersive delay is found to be

$$\tau_d = (2.4\ \mathrm{ns}) \left(\frac{l}{100\ \mathrm{m}}\right) \left(\frac{f}{100\ \mathrm{MHz}}\right)^{-1/2} . \qquad (16)$$

From Equation (10), we have $\kappa = 3.8 \times 10^{-7}\ \mathrm{m}^{-1}\ \mathrm{Hz}^{-1/2}$.

We now employ Equation (15) as the correction filter for a KSR200DB cable of length 150 m. The LWA1 beamformer operates at 196 million samples per second (MSPS). In the context of LWA1, the center frequency for the Taylor series expansion should be chosen to yield minimum frequency response error between 10 MHz and 88 MHz. By trying various frequencies over $10-88$ MHz, it is found that $f_c = 39.42$ MHz works well. To achieve peak phase error no larger than $1.0°$ over $10-88$ MHz, a 140-tap FIR filter is required using the prototype truncation method.

D. Reduction in the Order of Cable Correction Filter

The number of filter taps obtained using prototype truncation is quite large. Here, three alternative methods are considered: Kaiser windowing with $\beta = 5.65$ prior to truncation, Chebyshev windowing of sidelobe height -60 dB prior to truncation, and minimax optimization starting from the prototype of Section III-C. For the minimax optimization method described in Algorithm 1, the parameters are $\Delta M = 5$, $M_0 = 140$, $\epsilon = 0.01°$, $f_s = 196$ MHz, and $\Omega = 2\pi[10, 88] \times 10^6$ rad/s. In each approach, the required number of filter taps, M, is defined to be the minimum filter length which achieves phase accuracy of $1.0°$ over $10-88$ MHz. The results are shown in Figures 4(a)$-$4(c). The results illustrate that windowing techniques yield significantly less ripple, which is an advantage of that approach. However, minimax optimization yields a filter with much smaller filter length.

IV. Combination Scheme

It may not be practical or desirable to have separate FIR filters for cable correction and beamforming delay as shown in Figure 1. Here we consider combing these functions as shown in Figure 2.

The desired frequency response of the ideal combined filter is the product of the frequency response of individual filters; i.e., $H_i(\omega) = H_b(\omega) H_{cd}(\omega)$ where $H_b(\omega)$ is the frequency response of the delay FIR filter. The prototype for the combined filter can be obtained by taking the inverse Fourier transform of the desired frequency response and then using sampling and truncation. Then we can perform minimax optimization as described in Algorithm 1 and demonstrated in Section III-D.

Now we consider a combined filter including the functions of per-sensor cable correction and delay-and-sum beamforming. The cable correction filter is used to compensate the distortion in a KSR200DB cable of length 150 m as described in Section III-C. For a beamforming delay equal to 2.5 ns at the sample rate of 196 MSPS (i.e., about half period), the combined filter using the prototype truncation requires $M = 30$ to achieve peak phase error no larger than $1.0°$

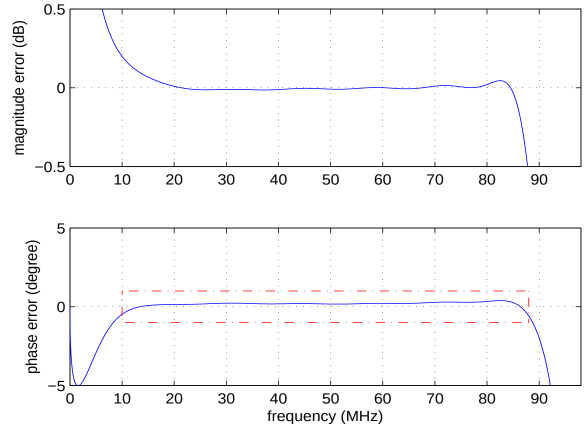

(a) Kaiser window ($M = 27$).

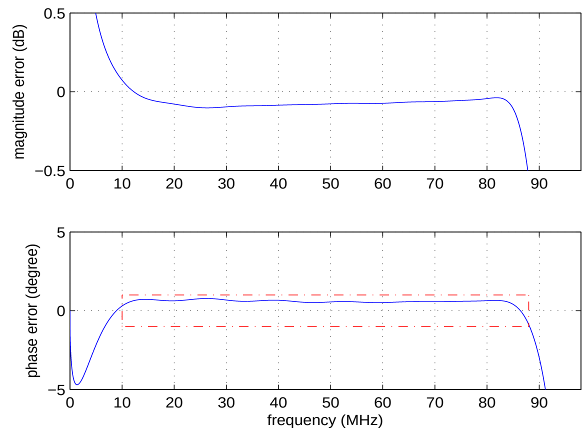

(b) Chebyshev window ($M = 29$).

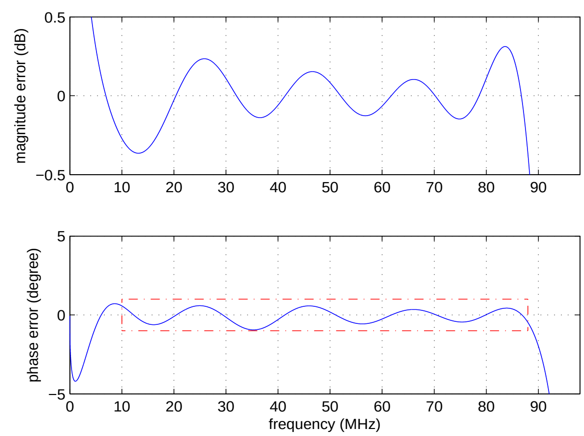

(c) Minimax optimization ($M = 19$).

Fig. 4. Performance of cable correction FIR filters using different design methods. In each figure, the top panel shows the error of magnitude response from the ideal, and the bottom panel shows the error of phase response from the ideal. The dash rectangular box in the bottom panel indicates the $1.0°$ phase error specification over $10-88$ MHz.

over $10 - 88$ MHz. Using $M_0 = 30$, $\Delta M = 2$, $\epsilon = 0.01°$, $f_s = 196$ MHz, and $\Omega = 2\pi[10, 88] \times 10^6$ rad/s, Algorithm 1 yields a 20-tap combined FIR filter, shown in Figure 5.

Since this result is likely dependent on the beamforming delay, we also consider a combined filter implementing a beamforming delay of 1.6 ns (i.e., about one third the sample period). The combined filter using prototype truncation requires $M = 82$ to achieve phase errors no larger than $1.0°$ over $10 - 88$ MHz. Using $M_0 = 82$, $\Delta M = 6$, $\epsilon = 0.01°$, $f_s = 196$ MHz, and $\Omega = 2\pi[10, 88] \times 10^6$ rad/s, Algorithm 1 yields a 28-tap combined FIR filter as shown in Figure 6.

V. Application to LWA1 Beamforming

In this section, we demonstrate our designs using a simplified version of LWA1 consisting of $N = 256$ isotropic sensors whose properties are identical over $10-88$ MHz. The arrangement of these sensors is shown in Figure 7. In the LWA1 cable system, lengths vary between 43 m and 149 m [12]. Cable losses and dispersive delays in the LWA1 array are shown in Figures 8 and 9, respectively, using Equations (9) and (10). Note that cable losses and dispersive delays are scattered over a large range, and vary significantly with frequency as well.

A. Calculation of SNR Improvement

System equivalent flux density (SEFD) is a commonly-used metric of the sensitivity of radio telescopes. SEFD is defined as the power flux spectral density, having units of W m^{-2} Hz^{-1}, which yields SNR equal to unity at the beamformer output. A method for calculation of SEFD using narrowband beamforming has already been described in [13]. Now we extend this to delay-and-sum (wideband) beamforming. Consider a delay-and-sum beamformer consisting of N sensors. Each sensor is followed by a M-tap delay FIR filter. Following [13],

$$\mathrm{SEFD} = \frac{2}{\eta} \frac{\mathbf{w}^H \left(\mathbf{R}_z + \mathbf{R}_u\right) \mathbf{w}}{\mathbf{w}^H \mathbf{R}_s \mathbf{w}} \ , \tag{17}$$

where η is impedance of free space, and following Figure 3,

$$\mathbf{w} = \left[w_{11} \ \cdots \ w_{N1} \ \cdots \ w_{1M} \ \cdots \ w_{NM}\right]^T \tag{18}$$

is the $NM \times 1$ column vector with the superscript "^{T}" being the transpose operation, and $\mathbf{R}_s$, $\mathbf{R}_z$, and $\mathbf{R}_u$ are the $NM \times NM$ covariance matrices associated with signal of interest, external noise, and internal noise, respectively.

Assuming the signal of interest is unpolarized and is wide-sense stationary, the desired signal covariance matrix is

$$\mathbf{R}_s = \mathbf{R}_s^{\theta\theta} + \mathbf{R}_s^{\phi\phi} \ , \tag{19}$$

where

$$\mathbf{R}_s^{\theta\theta} = \begin{bmatrix} \mathbf{A}_{\theta\theta} P_E^{\theta} & \cdots & \mathbf{A}_{\theta\theta} R_E^{\theta}[M-1] \\ \vdots & \ddots & \vdots \\ \mathbf{A}_{\theta\theta} R_E^{\theta}[M-1] & \cdots & \mathbf{A}_{\theta\theta} P_E^{\theta} \end{bmatrix} , \tag{20a}$$

$$\mathbf{R}_s^{\phi\phi} = \begin{bmatrix} \mathbf{A}_{\phi\phi} P_E^{\phi} & \cdots & \mathbf{A}_{\phi\phi} R_E^{\phi}[M-1] \\ \vdots & \ddots & \vdots \\ \mathbf{A}_{\phi\phi} R_E^{\phi}[M-1] & \cdots & \mathbf{A}_{\phi\phi} P_E^{\phi} \end{bmatrix} , \tag{20b}$$

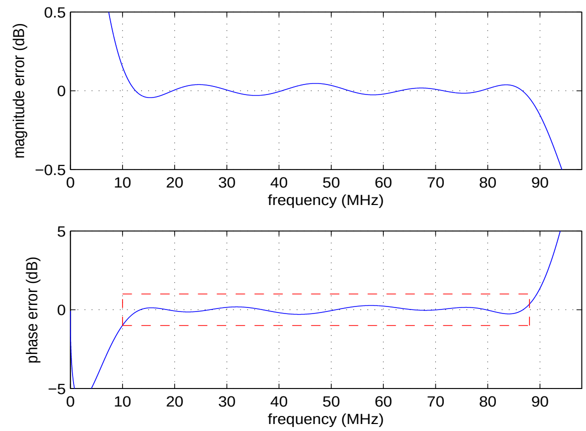

Fig. 5. Performance of the 20-tap combined (cable correction + delay) filter. The combined filter is used to simultaneously implement a delay equal to about one half sample period as well as compensation for loss and dispersion in a KSR200DB cable of length 150 m.

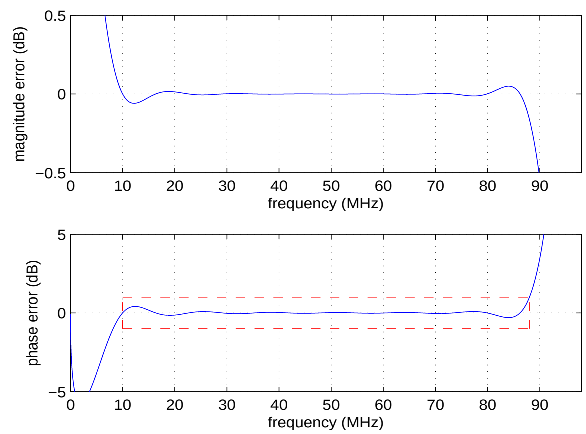

Fig. 6. Performance of the 28-tap combined (cable correction + delay) filter. The combined filter is used to simultaneously implement a delay equal to about one third sample period as well as compensation for loss and dispersion in a KSR200DB cable of length 150 m.

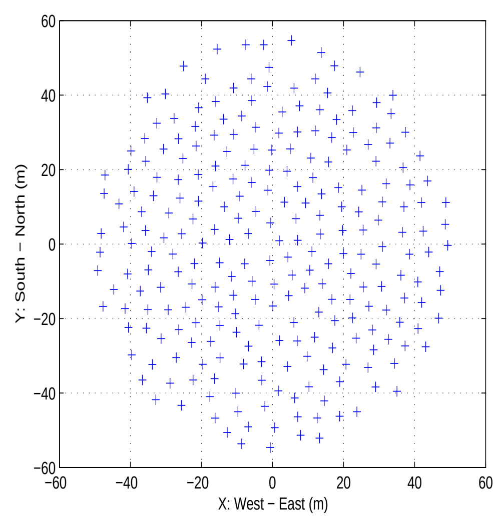

Fig. 7. Sensor arrangement in the LWA1 array [12]. The minimum distance between two sensors is 5 m.

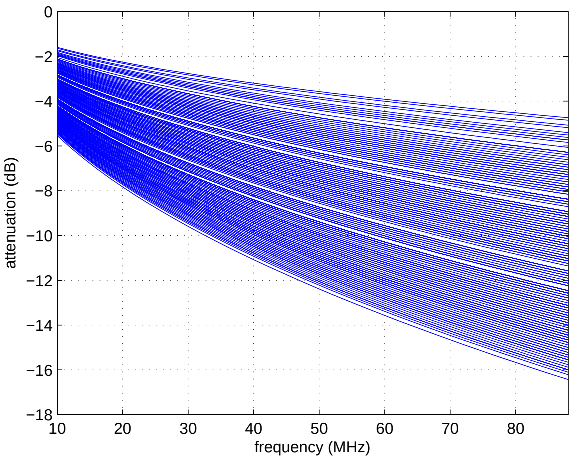

Fig. 8. Losses for all 256 cables.

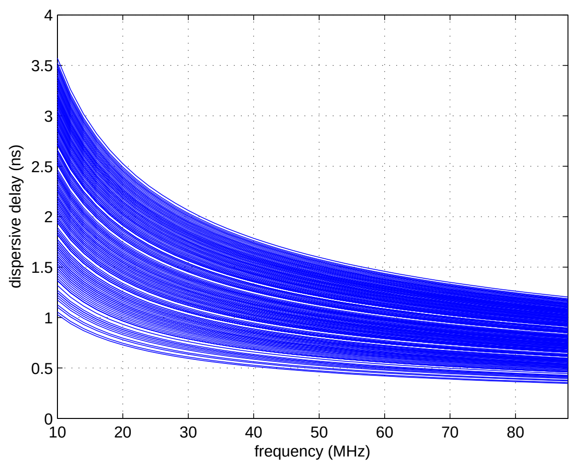

Fig. 9. Dispersive delays for all 256 cables.

$$\mathbf{A}_{\theta\theta} = \mathbf{a}_\theta^*(\psi_0)\mathbf{a}_\theta^T(\psi_0)\ , \quad \mathbf{A}_{\phi\phi} = \mathbf{a}_\phi^*(\psi_0)\mathbf{a}_\phi^T(\psi_0)\ , \tag{20c}$$

$$\mathbf{a}_\theta(\psi_0) = [a_1^\theta(\psi_0)\ a_2^\theta(\psi_0)\ \cdots\ a_N^\theta(\psi_0)]^T\ , \tag{20d}$$

$$\mathbf{a}_\phi(\psi_0) = [a_1^\phi(\psi_0)\ a_2^\phi(\psi_0)\ \cdots\ a_N^\phi(\psi_0)]^T\ , \tag{20e}$$

P_E^θ and P_E^ϕ are the powers of the θ- and ϕ-polarized components of the electric field of the signal of interest, $R_E^\theta[\cdot]$ and $R_E^\phi[\cdot]$ are the auto-correlation correlation functions of the desired signal, $a_n^\theta(\psi_0)$ and $a_n^\phi(\psi_0)$ are the effective lengths associated with the θ and ϕ polarizations for the n^{th} sensor for signals incident from ψ_0, and the superscript "*" is the conjugation operator. For this study, we assume isotropic sensors (i.e., $a_n^\theta(\psi) = a_n^\phi(\psi)$ are constant with respect to ψ) and we assume pattern multiplication applies; i.e., mutual coupling is ignored.

The external noise covariance matrix $\mathbf{R}_z$ can be partitioned into M^2 $N \times N$ submatrices as follows:

$$\mathbf{R}_z = \begin{bmatrix} \mathbf{P}_z & \cdots & \mathbf{P}_z R_z[M-1] \\ \vdots & \ddots & \vdots \\ \mathbf{P}_z R_z[M-1] & \cdots & \mathbf{P}_z \end{bmatrix}, \tag{21}$$

where $R_z[\cdot]$ is the auto-correlation function of external noise, and the $(n,n')^{\text{th}}$ $(n,n' = 1,\cdots,N)$ element of the $N \times N$ matrix $\mathbf{P}_z$ is the correlation of external noise between sensors n and n', which is given in [13] as

$$\mathbf{P}_z^{[n,n']} = \frac{k\eta}{\lambda^2}\int_{\phi=0}^{2\pi}\int_{\theta=0}^{\pi}\left[a_n^\theta(\psi)a_{n'}^\theta(\psi) + a_n^\phi(\psi)a_{n'}^\phi(\psi)\right]T_e(\psi)\sin\theta d\theta d\phi\ . \tag{22}$$

Here, k is Boltzmann's constant (1.38×10^{-23} J/K), λ is the wavelength, and $T_e(\psi)$ is the external noise brightness temperature in the direction ψ. In this study, we also assume that $T_e(\psi)$ is uniform over the sky ($\theta \leq \pi/2$) and zero for $\theta > \pi/2$, although in fact $T_e(\psi)$ varies considerably both as a function of ψ and a function of time of day due to the rotation of the Earth. This assumption provides a reasonable standard condition for comparing Galactic noise-dominated antenna systems, as explained in [14] and demonstrated in [15]. Using this model, $T_e(\psi)$ toward sky is found as a function of frequency; that is,

$$T_e(\psi) = \frac{1}{2k} I_v \frac{c^2}{f^2}\ , \tag{23}$$

where c is the speed of light in free space, f is frequency, and I_v is intensity having units of $\mathrm{W \cdot m^{-2} \cdot Hz^{-1} \cdot sr^{-1}}$ given by

$$I_v = I_g f_{\text{MHz}}^{-0.52} + I_{eg} f_{\text{MHz}}^{-0.80}\ , \tag{24}$$

where $I_g = 2.48 \times 10^{-20}$, $I_{eg} = 1.06 \times 10^{-20}$, and f_{MHz} is frequency in MHz.

The internal noise covariance matrix $\mathbf{R}_u$ can also be partitioned into M^2 $N \times N$ submatrices as

$$\mathbf{R}_u = \begin{bmatrix} \mathbf{P}_u & \cdots & \mathbf{P}_u R_u[M-1] \\ \vdots & \ddots & \vdots \\ \mathbf{P}_u R_u[M-1] & \cdots & \mathbf{P}_u \end{bmatrix}, \tag{25}$$

where $R_u[\cdot]$ is the auto-correlation function of internal noise, and $\mathbf{P}_u$ is an $N \times N$ diagonal matrix whose non-zero elements are given in [13] as

$$\mathbf{P}_u^{[n,n]} = kT_{p,n}R_L\ . \tag{26}$$

Here, $T_{p,n}$ is the input-referred internal noise temperature associated with the n^{th} sensor. For LWA1, it is reasonable to assume that all the electronics are identical such that $T_{p,n} = 250$ K. R_L is the impedance of load into which the antenna is terminated; that is, $R_L = 100\ \Omega$ for LWA1. Note we assume cable loss does not contribute significantly to $T_{p,n}$, which is the case for LWA1.

For a desired pointing direction 22° away from the zenith toward the east (i.e., $\theta = 22°$ and $\phi = 0°$), the resulting SEFD for a single sensor and for the beamforming array can be computed from Equation (17). The SNR improvement over that of a single stand by beamforming can thus be expressed as the ratio of the SEFD for a single stand to the SEFD for the beamformer.

B. Effect and Correction of Unequal Cable Distortion

Now we use the combination (cable dedispersion + beamforming delay) scheme and assess the improvement in SNR relative to beamforming without cable equalization. The per-sensor combined filter length is initially selected to be 28, which is what LWA1 actually has. Figures 10 and 11 show

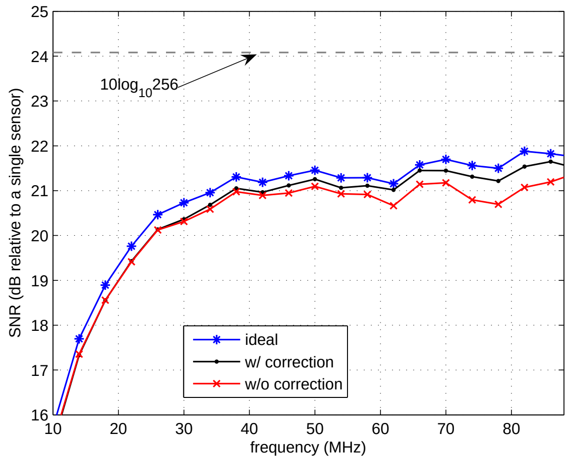

Fig. 10. Delay-and-sum beamforming performance in the different cases described in the text. 28-tap combined FIR filters are applied to each sensor.

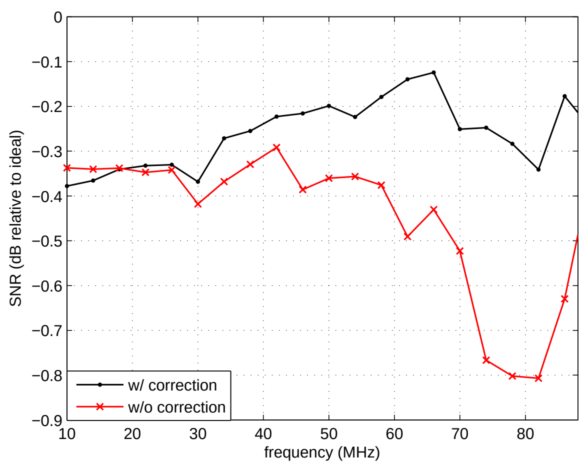

Fig. 11. Same as Figure 10, except now relative to the "ideal" result. 28 taps.

the SNR improvement over that of a single sensor by delay-and-sum beamforming in three different cases: (1) The ideal case where the effects of unequal cable distortion are either not significant or always perfectly compensated; (2) the realistic case where unequal cable losses and dispersive delays exist but with no correction implemented; and (3) same as (2) but now with correction. Note that all schemes experience severe degradation below 30 MHz; this is due to correlation of external noise between sensors, as explained in [13]. Also note that none of the results achieves the often-stated theoretical limit of SNR improvement equal to N, for the same reason. The results show that unequal cable losses (Figure 8) and dispersive delays (Figure 9) introduce an additional SNR performance penalty of $0.35-0.86$ dB if not corrected. Using the $M = 28$ per-sensor combined filters, we achieve a benefit of $0.05-0.45$ dB above 30 MHz. Note that there is a slight performance penalty (less than 0.05 dB) below 20 MHz, which is due to the insufficient filter length. For the same reason, the SNR performance with correction using combined FIR filters is still $0.10-0.40$ dB worse than the result in the case of ideal cables.

We now repeat the analysis using per-sensor combined FIR filters of different lengths to find the minimum M for which the SNR improvement by the combined filter is consistently better at all frequencies. It is found that $M = 42$ achieves this objective, as shown in Figure 12. (Note that the "w/o correction" results change slightly; this is because the length of the corresponding delay filters have also changed, even though the same delays are being implemented.) We repeat the analysis to find the minimum M for which the SNR degradation using combined filters is within 0.1 dB. Figure 13 shows $M = 58$ achieves this goal. These results confirm that the cable equalization scheme of Section III-B effectively mitigates the degradation in SNR due to unequal cable loss and dispersion, using filters of reasonable length.

Cable losses are easily equalized by varying the gains of the analog or digital receivers, which does not require digital filtering. Thus it is of interest to consider the benefit of correcting only loss. Here we consider two cases: (1) Perfect correction for cable losses only, which is equivalent to doing no correction on cables for which $\zeta = 0$; and (2) correction for cable losses at a given frequency; i.e., at all frequencies using the value for 50 MHz only. Figure 14 shows the result for $M = 58$. Note that significant improvement is possible using "loss-only" equalization. However, the performance is significantly less than that achieved when dispersion is also corrected. Interestingly, the results in the two cases are very close around 50 MHz and differences between the results become only slightly larger when the frequency is away from 50 MHz, which indicates that most of the benefit of "loss-only" correction can be obtained using "single frequency" correction.

VI. Conclusion

This paper has considered the effect of unequal loss and dispersion of coaxial cables on delay-and-sum beamforming arrays. A rigorous description of cable distortion was provided in Section III-A. A method for correcting and equalizing the distortion was developed in Sections III-B and III-D. A scheme for implementation of this method by modification of the coefficients of the same FIR filters used to implement beamforming delays (the "combination scheme") was developed in Section IV. In Section V we considered considered the problem in the context of the LWA1 radio telescope, and demonstrated that significant improvement is possible using our proposed equalization scheme. For LWA1, we found that uncorrected loss and dispersion results in SNR degradation between 0.35 dB and 0.86 dB from that achieved in the absence of cable distortion. This degradation can be made arbitrarily small, with the only limitation being filter length. For LWA1, it was found that 58-tap filters are required to reduce the degradation to less than 0.10 dB. We also demonstrated that significant improvement can be achieved by single-frequency correction of losses only, ignoring dispersion. In the case of LWA1, this simpler approach limits the degradation to about 0.24 dB.

Although these may seem to be only minor improvements, these are significant in the context of a large array. For

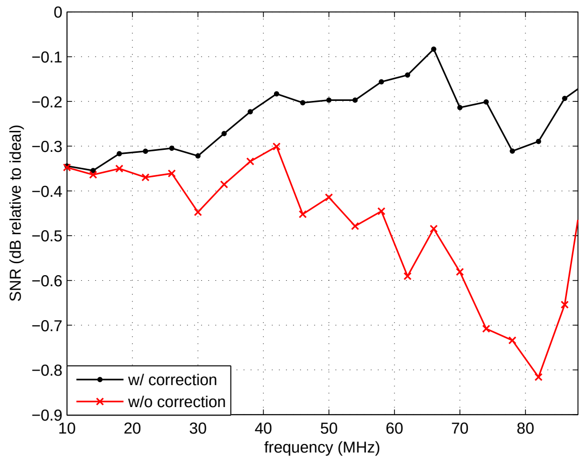

Fig. 12. Same as Figure 11, except for 42-tap per-sensor combined filters.

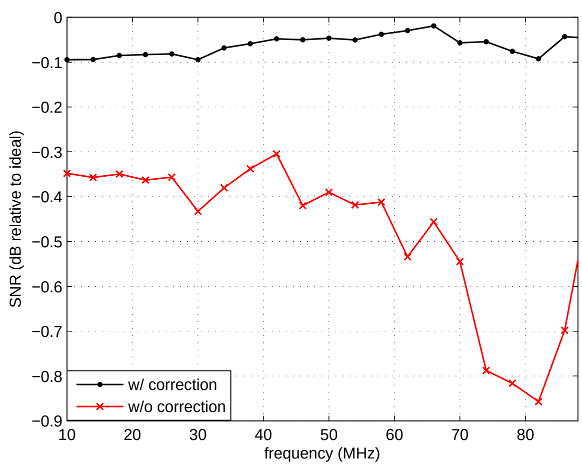

Fig. 13. Same as Figure 11, except for 58-tap per-sensor combined filters.

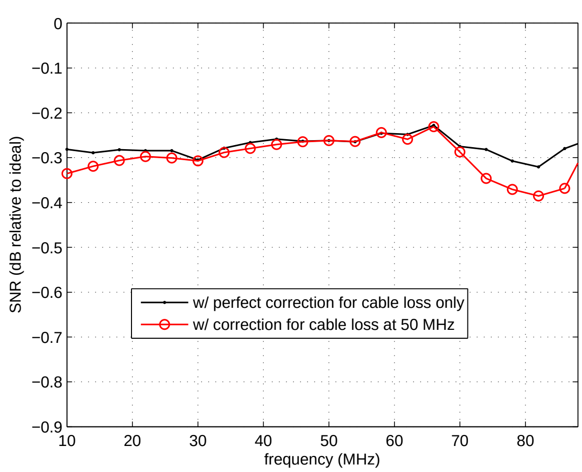

Fig. 14. Same as Figure 13, but now showing effect of "loss-only" corrections. 58 taps.

example, 0.3 dB improvement in SNR can be interpreted as 7% reduction in the number of antennas required. For LWA1, this corresponds to 17 fewer antenna pairs. Since a LWA station costs about US$800,000 [16] and the cost is approximately linear in the number of antennas, this amounts to a savings of about US$53,000 plus associated installation, power, and maintenance costs.

In this paper, we ignored antenna dispersion and the possibility of unequal dispersion between antennas due to mutual coupling. Further work should consider dispersion by antennas, which can in principle be corrected using a similar approach.

Finally, the theory and techniques described in Sections III and IV are applicable to a variety of systems which also potentially suffer from unequal cable losses and dispersive delays, including sonar arrays, HF/VHF band riometers, radar arrays, and other radio telescopes consisting of large numbers of low frequency antennas.

ACKNOWLEDGMENTS

This work was funded in part by the Office of Naval Research via contract N00014-07-C-0147 and in part by the National Science Foundation under award AST-1139963 of the University Radio Observatory program. The authors thank J. Craig and J. Hartman of University of New Mexico for providing measurements of KSR200DB cable.

APPENDIX

CHARACTERIZATION OF REALISTIC COAXIAL CABLES

Let a and b be the radii of the inner conductor and the facing surface of the outer conductor, respectively; σ_a and σ_b be the conductivities of the inner conductor and outer conductor, respectively; ϵ be the permittivity of the medium between the inner and outer conductor; and μ be the permeability of the medium between the inner and outer conductor. Typically, the shunt conductance is negligible for well-designed transmission line. Thus the propagation constant γ can be written as

$$\gamma = \sqrt{(R + j\omega L)(G + j\omega C)} \approx \sqrt{(R + j\omega L)j\omega C} \ . \quad (27)$$

The shunt capacitance per unit length is independent of frequency and is given in [11] as

$$C = \frac{2\pi\epsilon}{\ln(b/a)} \ . \quad (28)$$

The series inductance per unit length accounts for two sources of inductance and is given in [11] as

$$L = L_0 + L_{s0} \ , \quad (29)$$

where

$$L_0 = \frac{\mu}{2\pi} \ln\frac{b}{a} \quad (30)$$

is the ideal inductance associated with the magnetic component of the field between the conductors, and

$$L_{s0} = \frac{\mu^{1/2}}{4\pi^{3/2}} \left(\frac{\sigma_a^{-1/2}}{a} + \frac{\sigma_b^{-1/2}}{b} \right) f^{-1/2} \quad (31)$$

is the frequency-dependent inductance associated with the magnetic component of the field *interior* to the inner and outer conductors, due to the imperfect conductivity. The series resistance per unit length arises from the same current associated with L_{s0}. For good conductors, the real and imaginary parts of the wave impedance are equal; thus

$$R = 2\pi L_{s0} f \ . \tag{32}$$

Applying substitutions in Equation (27), we find

$$\gamma = j\beta_0 \sqrt{1 + (1-j)\frac{L_{s0}}{L_0}} \ , \tag{33}$$

where $\beta_0 = \omega\sqrt{L_0 C}$ is the wavenumber for an ideal coaxial cable. Note that any frequency dependence is due to the current interior to the conductors, which manifests as non-zero R and frequency-dependent L. The second term under the radical in Equation (33) is small compared to 1; see the example demonstrated in [17]. Applying the "small x" approximation $\sqrt{1+x} \approx 1 + \frac{1}{2}x$ to Equation (33), we obtain

$$\gamma \approx \beta_0 \frac{1}{2}\frac{L_{s0}}{L_0} + j\beta_0\left(1 + \frac{1}{2}\frac{L_{s0}}{L_0}\right) \ . \tag{34}$$

The real part of γ is then

$$\alpha = \mathrm{Re}\{\gamma\} = \beta_0 \frac{1}{2}\frac{L_{s0}}{L_0} \ , \tag{35}$$

and the imaginary part of γ is found to be

$$\beta = \mathrm{Im}\{\gamma\} = \beta_0\left(1 + \frac{1}{2}\frac{L_{s0}}{L_0}\right) \ . \tag{36}$$

After substituting Equations (35) and (36) into Equation (8) and applying some algebra, the cable distortion is found to be

$$\begin{aligned} H_c(\omega) &= \exp\left(-(1+j)\frac{\beta_0 l}{2}\frac{L_{s0}}{L_0}\right) \\ &= \exp\left[(1+j)\sqrt{\frac{\epsilon}{8}}\left(\frac{\delta_a^{-1/2}}{a} + \frac{\delta_b^{-1/2}}{b}\right)\left(\ln\frac{b}{a}\right)^{-1} l\sqrt{\omega}\right] \ . \end{aligned} \tag{37}$$

This is the physical description of the coaxial cable distortion, which depends only upon the geometry and materials of the cable.

We can also determine α and β directly from measurements: From (37), the attenuation in a coaxial cable of length l at frequency f can be modeled as

$$A = e^{-\alpha_0 l \sqrt{f/f_0}} \ , \tag{38}$$

where α_0 is the real part of the propagation constant specified at frequency f_0. The attenuation at any other frequency is $A = e^{-\hat{\alpha} l}$, where

$$\hat{\alpha} = \frac{\alpha_0}{\sqrt{2\pi f_0}}\sqrt{\omega} \ . \tag{39}$$

Also from Equation (37), the total delay in a cable of length l at frequency f can be modeled as

$$\tau = t_0 + t_1 \frac{l}{l_1}\left(\frac{f}{f_1}\right)^{-1/2} \ , \tag{40}$$

where the first term t_0 is the propagation delay in a dispersion-free cable, and the second term is the dispersive (excess) delay. Here, t_1 is the dispersive delay measured at frequency f_1 for length l_1. From Equation (6), we have

$$\hat{\beta} = \frac{1}{l}\int \tau_c \ d\omega = \frac{\omega t_0}{l} + \frac{t_1\sqrt{8\pi f_1}}{l_1}\sqrt{\omega} \ . \tag{41}$$

Since $\beta_0 l = \omega t_0$, we obtain

$$\hat{\beta} = \beta_0 + \frac{t_1\sqrt{8\pi f_1}}{l_1}\sqrt{\omega} \ . \tag{42}$$

The frequency response of the cable distortion then

$$\widehat{H}_c(\omega) = \exp\left[-\left(\frac{\alpha_0}{\sqrt{2\pi f_0}} + j\frac{t_1\sqrt{8\pi f_1}}{l_1}\right) l\sqrt{\omega}\right] \ . \tag{43}$$

A general expression for the frequency response of the distortion in a coaxial cable is thus

$$H_c(\omega) = e^{-(\zeta + j\kappa) l \sqrt{\omega}} \ , \tag{44}$$

where ζ and κ are constants, in m^{-1} $\mathrm{Hz}^{-1/2}$, dependent upon the physical parameters of the cable. For the case that $H_c(\omega)$ is determined from Equation (37), we have

$$\zeta = \kappa = \sqrt{\frac{\epsilon}{8}}\left(\frac{\delta_a^{-1/2}}{a} + \frac{\delta_b^{-1/2}}{b}\right)\left(\ln\frac{b}{a}\right)^{-1} \ . \tag{45}$$

For the case that $H_c(\omega)$ is determined from Equation (43), we have

$$\zeta = \frac{\alpha_0}{\sqrt{2\pi f_0}} \ , \quad \text{and} \quad \kappa = \frac{t_1\sqrt{8\pi f_1}}{l_1} \ . \tag{46}$$

In general, Equation (46) is more useful since perfect fit to actual cable response is guaranteed at least one frequency and the only assumption needed is that of $f^{1/2}$ dependence.

REFERENCES

[1] T. I. Laakso, *et al.*, "Splitting the unit delay: tools for fractional delay filter design," *IEEE Signal Processing Magazine*, vol. 13, pp. 30–60, Jan. 1996.

[2] T. L. Landecker, "A coaxial cable delay system for a synthesis radio telescope," *IEEE Transactions on Instrumentation and Measurement*, vol. 33, pp. 78–83, Jun. 1984.

[3] S. W. Ellingson, *et al.*, "The LWA1 radio telescope," *IEEE Transactions on Antennas and Propagation, submitted*. [online] available arXiv:1204.4816v1 [astro-ph.IM].

[4] W. M. Carey, "Sonar array characterization, experimental results," *IEEE Journal of Oceanic Engineering*, vol. 23, pp. 297–306, Jul. 1998.

[5] C. G. Little and H. Leinbach, "The riometer – a device for the continuous measurement of ionospheric absorption," *Proceedings of the IRE*, vol. 47, pp. 315–20, Feb. 1959.

[6] E. Brookner, "Phased array radars – past, present and future," *Radar*, pp. 104–13, Oct. 2002.

[7] C. J. Lonsdale *et al.*, "The murchison widefield array: design overview," *Proceedings of the IEEE*, vol. 97, pp. 1497–506, Aug. 2009.

[8] P. E. Dewdney *et al.*, "The square kilometre array," *Proceedings of the IEEE*, vol. 97, pp. 1482–96, Aug. 2009.

[9] A. W. Gunst and M. J. Bentum, "The LOFAR phased array system," in *2010 IEEE Symposium on Phased Array Systems and Technology (ARRAY)*, pp. 632–9, Oct. 2010.

[10] F. J. Harris, "On the use of windows for harmonic analysis with the discrete Fourier transform," *Proceedings of the IEEE*, vol. 66, pp. 51–83, Jan. 1978.

[11] W. H. Hayt, Jr., and J. A. Buck, *Engineering Electromagnetics*. Boston: McGraw-Hill Higher Education, 7th ed.

[12] S. Ellingson, J. Craig, and J. Hartman, "LWA-1 antenna position and cable data, Ver. 3," Long Wavelength Array Memo 170, Dec. 9, 2010. [Online] Available: http://www.ece.vt.edu/swe/lwa/.

[13] S. W. Ellingson, "Sensitivity of antenna arrays for long-wavelength radio astronomy," *IEEE Transactions on Antennas and Propagation*, vol. 59, pp. 1855–63, Jun. 2011.

[14] S. W. Ellingson, "Antennas for the next generation of low-frequency radio telescopes," *IEEE Transactions on Antennas and Propation*, vol. 53, pp. 2480–9, Aug. 2005.

[15] S. W. Ellingson, J. H. Simonetti, and C. D. Patterson, "Design and evaluation of an active antenna for a 29-47 MHz radio telescope array," *IEEE Transactions on Antennas and Propagation*, vol. 55, pp. 826–31, Mar. 2007.

[16] S. W. Ellingson, *et al.*, "The long wavelength array," *Proceedings of the IEEE*, vol. 97, pp. 1421–30, Aug. 2009.

[17] S. W. Ellingson, "Dispersion in coaxial cables," memo 136, Jun. 1, 2008. Long Wavelength Array Memo Series [online]. Available: http://www.ece.vt.edu/swe/lwa/.